water

MDPI

Article

Integrating Satellite Rainfall Estimates with Hydrological Water Balance Model: Rainfall-Runoff Modeling in Awash River Basin, Ethiopia

Girma Berhe Adane [1], Birtukan Abebe Hirpa [1], Belay Manjur Gebru [2], Cholho Song [3] and Woo-Kyun Lee [3,4,*]

[1] Haramaya Institute of Technology, School of Water Resource and Environmental Engineering, Haramaya University, Dire Dawa 138, Ethiopia; girma.berhe@haramaya.edu.et (G.B.A.); birtukan.abebe@haramaya.edu.et (B.A.H.)
[2] Ecology and Environmental Policy, Tigray Institute of Policy Research and Studies, Mekelle 902, Ethiopia; belaymg7@gmail.com
[3] OJEong Resilience Institute (OJERI), Korea University, Seoul 02841, Korea; cholhosong@korea.ac.kr
[4] Division of Environmental Science and Ecological Engineering, Korea University, Seoul 02841, Korea
* Correspondence: leewk@korea.ac.kr

Abstract: Hydrologic models play an indispensable role in managing the scarce water resources of a region, and in developing countries, the availability and distribution of data are challenging. This research aimed to integrate and compare the satellite rainfall products, namely, Tropical Rainfall Measuring Mission (TRMM 3B43v7) and Precipitation Estimation from Remotely Sensed Information using Artificial Neural Networks-Climate Data Record (PERSIANN-CDR), with a GR2M hydrological water balance model over a diversified terrain of the Awash River Basin in Ethiopia. Nash–Sutcliffe efficiency (*NSE*), percent bias (*PBIAS*), coefficient of determination (R^2), and root mean square error (*RMSE*) and Pearson correlation coefficient (*PCC*) were used to evaluate the satellite rainfall products and hydrologic model performances of the basin. The satellite rainfall estimations of both products showed a higher *PCC* (above 0.86) with areal observed rainfall in the Uplands, the Western highlands, and the Lower sub-basins. However, it was weakly associated in the Upper valley and the Eastern catchments of the basin ranging from 0.45 to 0.65. The findings of the assimilated satellite rainfall products with the GR2M model exhibited that 80% of the calibrated and 60% of the validated watersheds in a basin had lower magnitude of *PBIAS* (<±10), which resulted in better accuracy in flow simulation. The poor performance with higher *PBIAS* (≥±25) of the GR2M model was observed only in the Melka Kuntire (TRMM 3B43v7 and PERSIANN-CDR), Mojo (PERSIANN-CDR), Metehara (in all rainfall data sets), and Kessem (TRMM 3B43v7) watersheds. Therefore, integrating these satellite rainfall data, particularly in the data-scarce basin, with hydrological data, generally appeared to be useful. However, validation with the ground observed data is required for effective water resources planning and management in a basin. Furthermore, it is recommended to make bias corrections for watersheds with poorlyww performing satellite rainfall products of higher *PBIAS* before assimilating with the hydrologic model.

Keywords: TRMM 3B43v7; PERSIANN-CDR; GR2M Hydrologic Model; Awash River Basin

check for updates

Citation: Adane, G.B.; Hirpa, B.A.; Gebru, B.M.; Song, C.; Lee, W.-K. Integrating Satellite Rainfall Estimates with Hydrological Water Balance Model: Rainfall-Runoff Modeling in Awash River Basin, Ethiopia. *Water* **2021**, *13*, 800. https://doi.org/10.3390/w13060800

Academic Editor: David Dunkerley

Received: 16 February 2021
Accepted: 12 March 2021
Published: 15 March 2021

Publisher's Note: MDPI stays neutral with regard to jurisdictional claims in published maps and institutional affiliations.

Copyright: © 2021 by the authors. Licensee MDPI, Basel, Switzerland. This article is an open access article distributed under the terms and conditions of the Creative Commons Attribution (CC BY) license (https://creativecommons.org/licenses/by/4.0/).

1. Introduction

To address water resource planning and management problems, different rainfall-runoff models are used to understand the hydrological processes in a basin. However, it is necessary to test whether a specific model fits a particular basin [1,2]. The applicability of these models is mainly constrained by the type and availability of input data in specific basins. The availability and distribution of ground-based rainfall-runoff data in African river basins are sparse [3]. This makes hydrological studies difficult in a basin where gauging stations are poorly distributed, particularly in the river basins of Ethiopia [4,5].

The Awash River Basin (ARB) has a complex landscape, varied climatic conditions, and an uneven distribution of hydrometeorological stations [6,7]. Rapid population growth, settlement, expansion of agricultural activities, upstream soil erosion, and pollutants in the basin threaten the freshwater resource availability of the ARB [8–10].

There are policy challenges on implementation of integrated water resource management (IWRM) principles in ARB. Adey et al. [11] have made an in-depth insight on IWRM policies and practices on a basin. They explained that there is a considerable disagreement on IWRM principles and the approach followed in a river basin. This has resulted in poor water management practices and scarcity of freshwater resource in a basin among different water users. Therefore, different water resource management and planning tools need to be synchronized to improve the implementation of IWRM on a river basin.

Various studies worldwide have used conceptual lumped hydrologic models to estimate the regional water availability for an ungauged basin [12–14]. Others have also used this type of model to assess the climatic impacts on different hydrological conditions [4,5,15,16]. Among different hydrologic models, the GR2M water balance model is tested in ARB.

The GR2M water balance model is similarly categorized as a global conceptual rainfall-runoff model. It is a monthly lumped hydrological model characterized by its parsimonious and low-level complexity. Furthermore, it is mainly focused on prominent features of the rainfall-flow transformation. This model is valuable for managing water resources, reservoir simulation, and drought predictions. In addition, Coron et al. [17] explained that GR lumped hydrological models are suitable for flood forecasting and impact assessment on climate change.

The GR2M model is widely evaluated in different parts of the world, for example, in France [18,19], Peru [20,21], Southeast Asia [22], Iran [23], Algeria [24,25], Benin [26], and Burkina Faso [27]. This demonstrates that the GR2M model has the greatest potential to be used in specific environments.

In Ethiopia, different studies have been conducted using hydrologic models over various catchments or at the river basin scale. Tadesse and Dai [28] predicted sedimentation in reservoirs by combining catchment-based (Soil and Water Assessment Tool (SWAT)) and stream-based (Hydrologic Engineering Center-River Analysis System (HEC-RAS)) models to estimate the sediment load reaching the Koka reservoir in the Upper Awash Basin, Ethiopia. Furthermore, Setegn et al. [29] and Mekonnen et al. [30] tested the selected catchment of the Upper Blue Nile using the SWAT model. Uhlenbrook et al. [31] analyzed the catchment behavior of the Upper Blue Nile catchment using Hydrologiska Byråns Vattenbalansavdelning (HBV) modeling. In the same basin, Abdo et al. [32] assessed the climate change influences on the hydrology of Gilgel Abay watershed using the HBV model.

Hydrometeorological data play a significant role for hydrologic modeling purposes to manage the water resources in a basin [33]. The rainfall gauging station distribution map of Ethiopia shows that the concentration of gauging stations is relatively high in the Uplands and Western highlands of the river basin, but the stations are sparsely distributed in the Upper valley, Middle valley, Eastern catchment, and Lower basin [34]. The adequacy and quality of recorded hydrometeorological data in a basin remain a challenge in hydrology and water resource-related studies in the ARB [35]. Therefore, testing and integrating satellite rainfall products with the available flow data greatly improves the applicability of any hydrological model that associates the rainfall-runoff relations, and also offers an alternative to ground-based rainfall estimates in an area where no records of observed rainfall are available [20,36,37].

To date, various studies related to satellite rainfall products over Ethiopia's river basins have been conducted, and the abilities of the products to detect rain events have been tested [3,6,35,38,39]. However, integrating these satellite rainfall products with the GR2M water balance model has never been tested in the Ethiopian river basin. Furthermore, research on integrating satellite rainfall products with hydrological models to study the rainfall-runoff process at a large river basin scale is scarce. This study provides insights on

the rainfall-runoff modeling using different satellite rainfall (Tropical Rainfall Measuring Mission (TRMM) 3B43 and Precipitation Estimation from Remotely Sensed Information using Artificial Neural Networks-Climate Data Record (PERSIANN-CDR)) products with a GR2M hydrologic water balance model in the water-stressed ARB of Ethiopia.

2. Data and Methods

2.1. Study Area

The Awash River is one of the largest rivers within Ethiopian territories. It is located at 7°53′ N–12° N and 37°57′ E–43°25′ E and covers an area of 116,373 km^2. The elevation in the river basin ranges from 240 to 4187 m above sea level (m a.s.l.) (Figure 1). Based on the hydrologic conditions of the ARB, it has been classified into seven sub-basins, which are the Uplands (Holeta, Melka Kuntire, Hombole, and Mojo areas), the Upper valley (Sire and Metehara areas), the Western highlands (Kessem Kebena areas), the Middle valley (Adaitu area), the Lower valley, and Lower plain. These Lower valley and Lower plain is considered as Lower basin (Tendaho sub-basin). The Western highlands has a major contribution to the surface flow of the river basin [40,41].

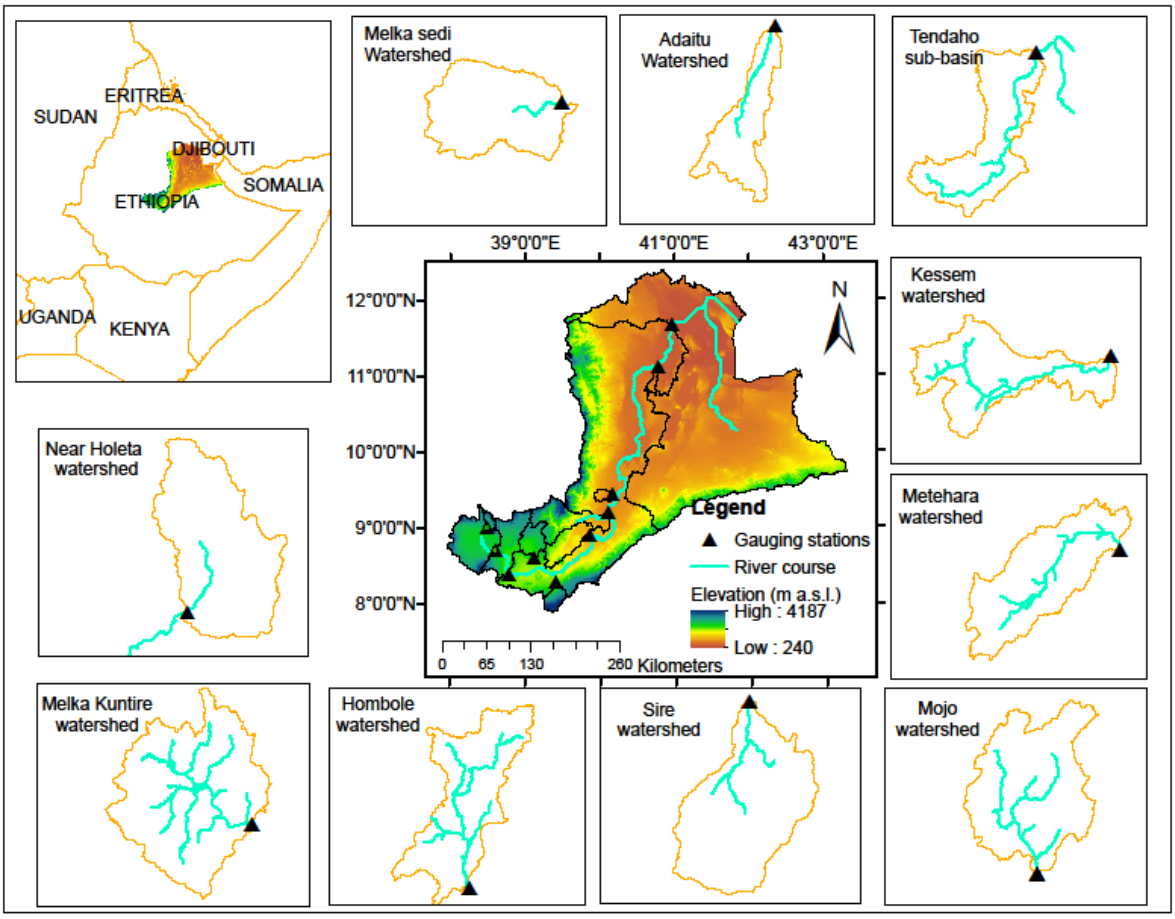


Figure 1. Gauging stations, elevation, and stream networks of the Awash River Basin (ARB) in Ethiopia.

The average annual rainfall of the ARB varies from 160 (in Asaita of the Lower plain sub-basin) to 1600 mm at Ankober (the Western highland sub-basin). Additionally, mean annual temperature of the ARB ranges from 20.8 to 29 °C at Koka (in the Upland sub-basin) and Dubti (in the Lower valley sub-basin), respectively [42]. The major land use land cover proportionate of the basin includes agricultural land (51.39%), grassland (29.79%), and shrublands (8.11%), respectively [40]. A climatic data summary of the ARB is provided in Table 1.

Table 1. Summary of climatic data of the ARB in Ethiopia.

River	Stations	Lat. (°N)	Long. (°E)	Altitude (m a.s.l.)	RF (mm/yr)	T_{mean} (°C)	RH_{mean} (%)	Length of Record
Holeta	Holeta	9.00	38.49	2221	1167.8	16.9	60.3	1998–2010
Awash	Melka Kuntire	8.71	38.60	2003	1007.1	25.3	38.8	1998–2009
Awash	Homboloe	8.38	38.78	1709	897.5	19.6	49.6	1998–2010
Mojo	Mojo	8.61	39.12	1772	1011.8	19.9	48.6	1998–2010
Keleta	Sire	8.29	39.40	1595	1116.5	18.8	56.9	1998–2010
Awash	Metehara	8.90	39.85	754	610.0	27.3	39.6	1998–2009
Kessem	Awara Melka	9.20	40.10	763	673.5	25.3	38.8	1998–2010
Awash	Melka sedi	9.44	40.15	732	567.1	27.3	40.5	1998–2010
Awash	Adaitu	11.13	40.78	505	527.7	30.9	32.7	1998–2010
Awash	Tendaho	11.68	40.96	411	213.0	30.3	32.7	1998–2010

2.2. Data Sources

The delineation of the sub-basins for selected stations and the whole river basin was performed using a 90 m resolution digital elevation model of Shuttle Radar Topographic Mission (SRTM) downloaded from the United States Geological Survey (USGS) website (https://earthexplorer.usgs.gov/ accessed on 10 January 2020).

The daily rainfall data (41 stations) and other climatic parameters (daily minimum and maximum temperature, wind speed, relative humidity, sunshine hour duration) for 10 sub-basins were obtained from the national meteorology agency of Ethiopia. The satellite rainfall products (TRMM 3B43v7 and PERSIANN-CDR) with spatial resolution of 0.25° × 0.25° (~27.8 × 27.8 km) were retrieved from the data center of US National Aeronautics and Space Administration (NASA, http://giovanni.gsfc.nasa.gov/giovanni/ accessed on 5 March 2020) and Center for Hydrometeorology and Remote sensing (http://chrsdata.eng.uci.edu/ accessed on 15 March 2020) for the length of records described in Table 1, respectively. These daily data were used to compute the monthly and annual climatic parameters depending on the needs of the analyses and in accordance with the available monthly discharge data of a river in a basin.

2.3. Preliminary Data Analysis

The missing observed rainfall data for long-term daily average values of various years were infilled if the missing data were less than 20% of the total. In addition, some missing rainfall data were replaced from the corresponding stations that had similar hydrometeorological characteristics. However, data with continuous missing values were systematically ignored from the analysis. There were no missing data for monthly satellite rainfall products of the sub-basins.

A Tukey fence method was used to test the outliers that can affect the detection of inhomogeneity of rainfall data series [43,44]. The rainfall data range is explained below.

$$[Q_1 - 1.5 \times IQR,\ Q_3 + 1.5 \times IQR], \quad (1)$$

where Q_1 and Q_3 are the upper and lower quartile points, respectively, 1.5 refers to the standard deviation from the mean, and IQR are the interquartile ranges.

The consistency of the observed rainfall data was analyzed using double-mass curve techniques [43,45] for only 10 meteorological stations with river flow data. A Theissen polygon method was used to convert point rainfall to areal rainfall for specific sub-basins that had river flow records. For comparison, mean multi-annual isohyetal rainfall maps over the entire basin using the observed and satellite rainfall were analyzed using kriging techniques to compare the patterns and ranges of rainfall. Similarly, the monthly potential evapotranspiration (PET) for the study period, for 10 river gauging stations, were performed using the Penman–Monteith (CROPWAT 8.0 software) and Blaney–Criddle methods depending on the climatic data availability.

For this study, the monthly river flow data (discharge, m^3/s) were obtained from the Global Runoff Data Center (GRDC, http://www.bafg.de/GRDC/ accessed on 17 December

2019) and Ministry of Water, Irrigation, and Electricity of Ethiopia (MoWIE).

ArcMap 10.1 and ArcSWAT were used for delineating and extracting the river networks, determining the basin area, and other basin characteristics. In addition, an elevation map, soil water holding capacity maps, and interpolation of point rainfall data using kriging were analyzed using Arc Map 10.1. MATLAB R2020a and Microsoft Excel 2016 were used for statistical analysis and graph development.

2.4. Methods

2.4.1. Soil Water Holding Capacity (SWHC)

The SWHC represents a soil moisture reserve in a soil which is being utilized for growing of vegetations in water deficit periods when rainfall does not meet the crop evapotranspiration demands [46,47]. The soil map of the river basin was prepared using FAO soil database as information. These 14 soil groups have a distinct proportionate of soil textural classes. Therefore, field capacity (*FC*) and permanent wilting point (*PWP*) ranges of values of a dominant texture of soil types were extracted from Allen et al. [48]. In addition, depth of the root zone of dominant crops in various parts of the river basin was used as input to compute the total available water (*TAW* or SWHC). This information was later used as an input to estimate the initial filling rate of the two tanks assumed in the GR2M conceptual model. Figure 2 shows the soil map of the ARB that is dominated by 14 soil groups. The textural classes of each soil group were identified from harmonized world soil database (HWSD) documents [49].

$$TAW = 1000 \times (\theta_{FC} - \theta_{PWP}) \times Z_r, \quad (2)$$

where *TAW* is total available water, which is equal to SWHC, Z_r is the depth of root zone (m), θ_{FC} and θ_{PWP} is the soil moisture at field capacity and wilting point (m^3 m^{-3}), respectively.

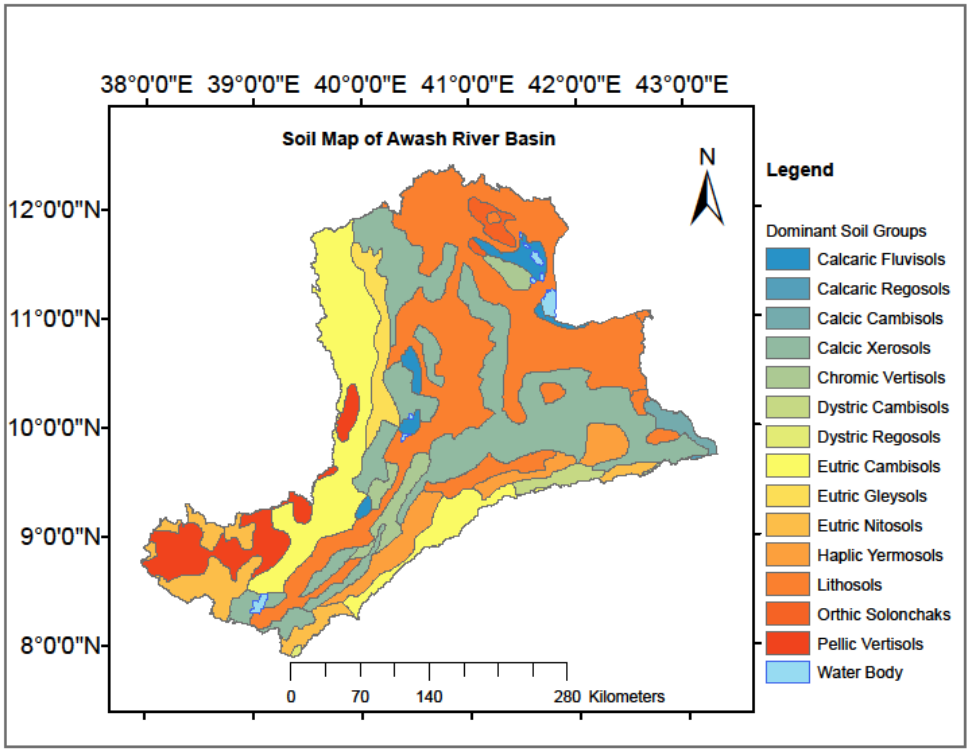


Figure 2. Soil map of the ARB in Ethiopia.

2.4.2. GR2M Hydrological Modeling

The GR2M is a spatially lumped hydrologic model with two-parameter estimation from a monthly time-step input data of a given basin [19,50,51]. The general concept, scheme, and detailed formula of the GR2M model are explained in [50]. Here, this GR2M hydrologic model was used to calibrate and validate in ARB using different rainfall data sets.

2.4.3. Satellite Rainfall and Hydrological Model Evaluation Criteria

The data records from each sub-basin were categorized into two different periods—for calibration and simulation of flows. These periods varied depending on the length of available data for each sub-basin. The first year of simulated discharge, which considered a warmup period, was not used in computations of performance evaluation of the model.

Different statistical methods were used as the basis for hydrometeorological evaluation. Among these model evaluation criteria, Nash–Sutcliffe efficiency (*NSE*), percent bias (*PBIAS*), coefficient of determination (R^2), Pearson correlation coefficient (*PCC*), and root mean square error (*RMSE*)-observation standard deviation ratio (*RSR*) are commonly used [21,52–54]. These criteria are indicated below.

$$NSE = 1 - \frac{\sum_{i=1}^{n} (Q_{obs,i} - Q_{sim,i})^2}{\sum_{i=1}^{n} (Q_{obs,i} - \overline{Q_{obs}})^2}, \quad (3)$$

$$PBIAS = \left[\frac{\sum_{i=1}^{n} (Q_{obs,i} - Q_{sim,i})}{\sum_{i=1}^{n} (Q_{obs,i})} * 100 \right], \quad (4)$$

$$R^2 = \left(\frac{\sum_{i=1}^{n} (Q_{obs,i} - \overline{Q_{obs}})(Q_{sim,i} - \overline{Q_{sim}})}{\sqrt{\sum_{i=1}^{n} (Q_{obs,i} - \overline{Q_{obs}})^2} \sqrt{\sum_{i=1}^{n} (Q_{sim,i} - \overline{Q_{sim}})^2}} \right)^2, \quad (5)$$

$$PCC = \frac{Cov\ (P^{Sat}, P^{Gauge})}{\sqrt{Var(P^{Sat})} \sqrt{Var(P^{Gauge})}}, \quad (6)$$

$$RSR = \frac{RMSE}{STDEV_{obs}} = \frac{\left[\sqrt{\sum_{i=1}^{n} (Q_{obs,i} - Q_{sim,i})^2} \right]}{\left[\sqrt{\sum_{i=1}^{n} (Q_{obs,i} - \overline{Q})^2} \right]}, \quad (7)$$

where $Q_{obs,i}$ is the ith observed value, $Q_{sim,i}$ is the ith simulated value, $\overline{Q_{obs}}$ is the mean observed value, and n is the total number of observations, $\overline{Q_{sim}}$ is the mean simulated value, P_i^{Gauge} and P_i^{Sat} are annual or monthly on-site observed rainfall (gauged) and satellite rainfall estimates, $STDEV_{obs}$ is the observed standard deviation. The ratings of the evaluation criteria were performed as shown in Table 2.

Table 2. General performance ratings for a hydrologic model [52].

Performance Rating	*RSR*	*NSE*	*PBIAS* (%)
Very good	$0.00 \leq RSR \leq 0.50$	$0.75 \leq NSE \leq 1.00$	$PBIAS < \pm 10$
Good	$0.50 < RSR \leq 0.60$	$0.65 < NSE \leq 0.75$	$\pm 10 \leq PBIAS < \pm 15$
Satisfactory	$0.60 < RSR \leq 0.70$	$0.50 < NSE \leq 0.65$	$\pm 15 \leq PBIAS < \pm 25$
Unsatisfactory	$RSR > 0.70$	$NSE \leq 0.50$	$PBIAS \geq \pm 25$

3. Results and Discussion

3.1. Comparison of Satellite Rainfall with Observed Rainfall

The isohyetal rainfall maps using ordinary kriging methods were developed (Figure 3). In addition, comparisons of the satellite (TRMM 3B43v7 and PERSIANN-CDR) and observed rainfall data were performed using statistical descriptors such as *PCC* and *RMSE* (Figure 4).

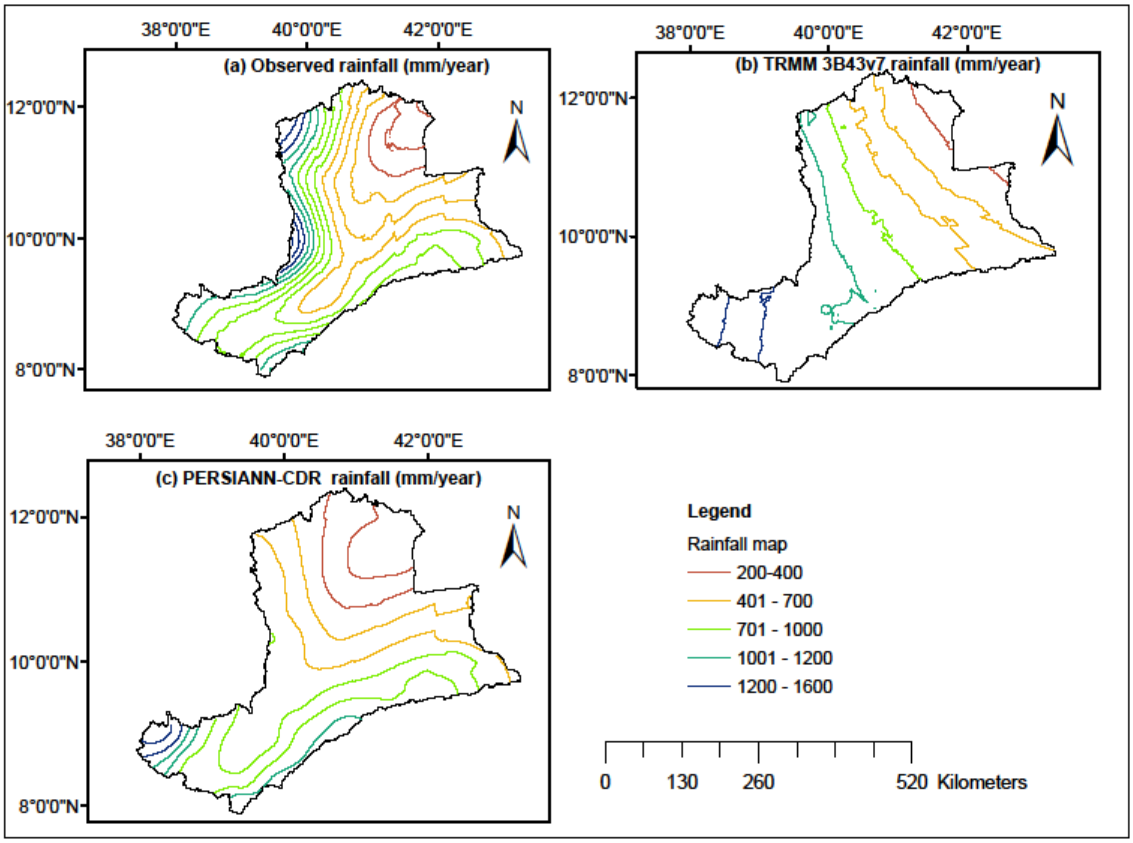


Figure 3. (**a**–**c**) Isohyetal rainfall map using kriging of mean multiannual rainfall records generated with different data sources.

Isohyetal rainfall (Figure 3) shows that the observed rainfall captured a wider range of rainfall amounts on a yearly basis, with a minimum of 242 in the Lower Awash basin and a maximum of 1536 mm in the Western highland catchment (Table 3). However, the satellite rainfall estimates in a basin captured nearly the same minimum rainfall amount per year for both products, but showed a discrepancy in the maximum ranges of rainfall records in TRMM 3B43v7 (1185 mm) and PERSIANN-CDR (1457 mm) (Table 3).

Table 3. Satellite products and ground observed rainfall ranges.

Rainfall Type	* RF_{min} (mm)	RF_{max} (mm)
Observed	242	1536
TRMM 3B43v7	430	1185
PERSIANN-CDR	413	1457

* RF designated as rainfall.

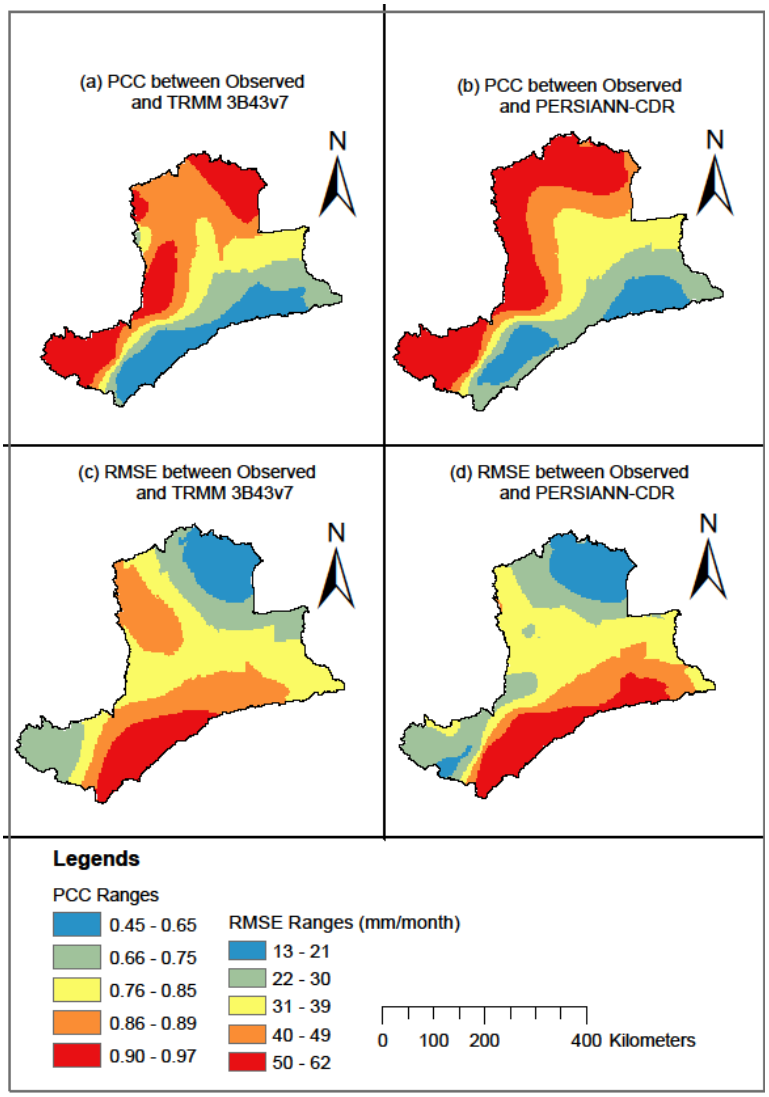


Figure 4. (**a**–**d**) Pearson correlation coefficient (*PCC*) and root mean square error (*RMSE*) between observed and satellite monthly rainfall data.

The isohyetal pattern of rainfall showed a resemblance between the observed and PERSIANN-CDR data, but it was completely different in the TRMM 3B43v7 product. This variation might be due to the nature of the product produced, the elevation, and rainfall regime of the basin.

Both satellite rainfall estimations showed a higher *PCC* with areal observed rainfall in the Uplands, the Western highlands, and the Lower sub-basins. However, it was weakly associated in the Upper valley and the Eastern catchments of the basin (Figure 4). A higher *RMSE* was noted in the Upper valley area of the basin for both satellite rainfall data, and it extended into the Eastern catchment while using PERSIANN-CDR. The long-term annual PERSIANN-CDR rainfall with station elevation showed a decreasing trend, particularly in the highest elevation areas (2250–2800 m). The elevations of the selected river gauging stations were located below 2250 m. Therefore, it was possible to apply the two-satellite data depending on the location and altitude of the basin.

3.2. SWHC/TAW

Using the soil groups and textural information, the *TAW* in the soil of various ranges, such as minimum, maximum, and mean values, were computed. The *TAW* maps for the soil group in ARB are shown in Figure 5.

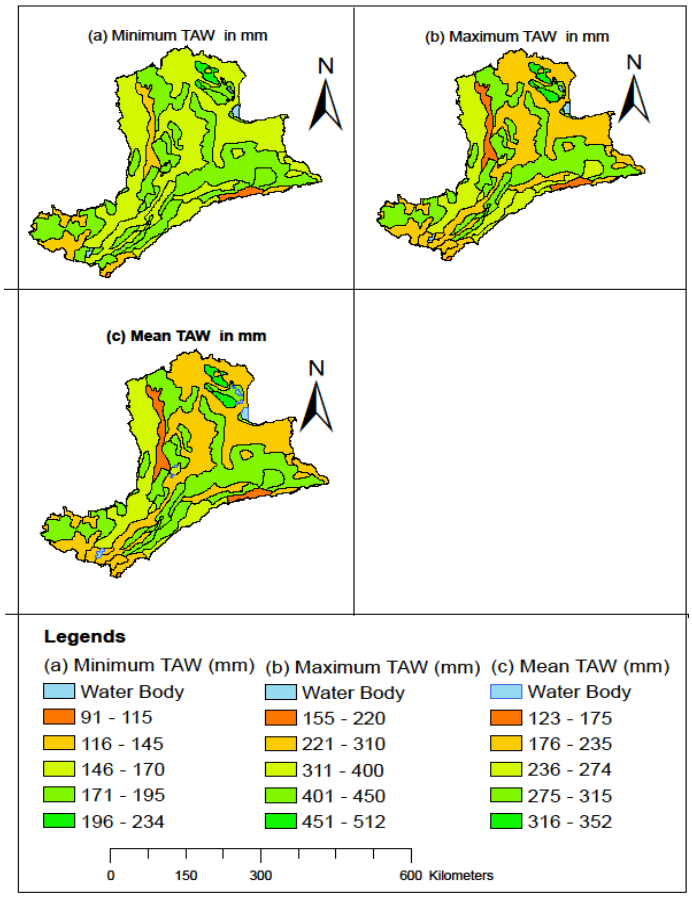


Figure 5. (**a**–**c**) Total available water (*TAW*) maps for different soil groups in ARB.

The Uplands, the Western highland catchments, and the Eastern catchments were dominated by higher *TAW* in the root zone (Figure 5). In contrast, less available water was observed in the Middle Awash and Lower Awash sub-basins.

3.3. GR2M Hydrological Modeling

The areal ground rainfall observation stations (GROS) generated using the Thiessen polygon for the sub-basins were compared with the areal satellite rainfall data of individual stations in the ARB. The comparison was based on the different statistical evaluation criteria discussed below.

3.3.1. Relationship of Mean PET, Streamflow vs. Rainfall

The mean annual PET trends in the basin showed a 54 mm drop for every increment of 50 mm rainfall in the basin, and PET was negatively correlated (−1.07) with mean rainfall in the basin. In addition, other climatic factors may influence the PET of the ARB. The mean annual rainfall trends exhibited a high coefficient of determination (R^2 = 0.81) with a mean streamflow rise of 14 mm for every 50 mm increment of rainfall (Figure 6).

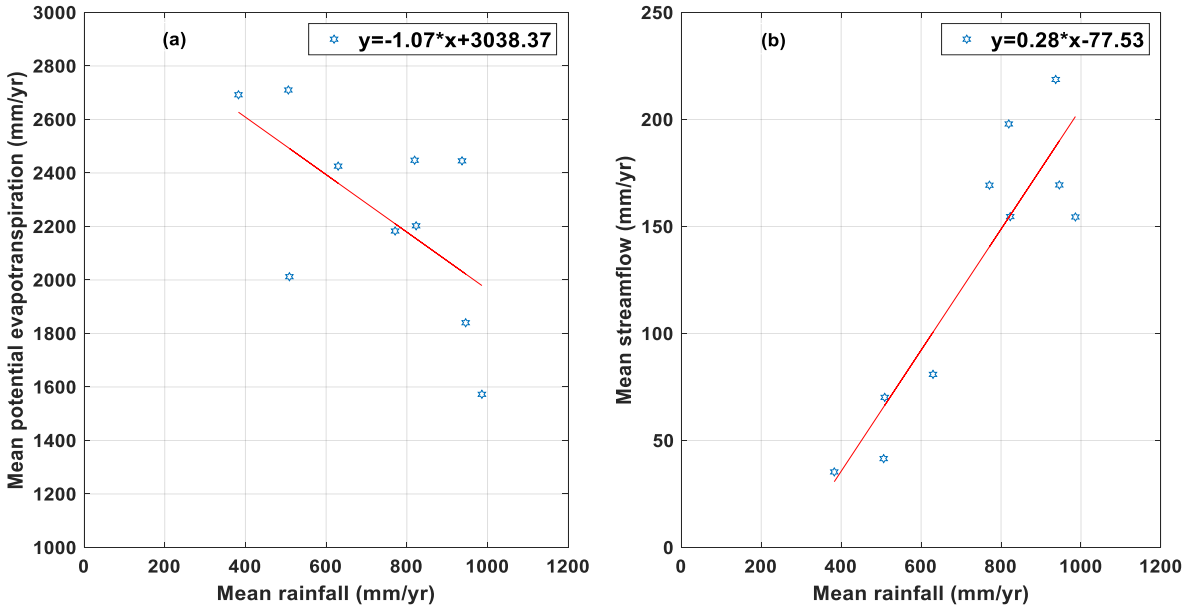


Figure 6. (**a**) Mean potential evapotranspiration (PET) versus mean rainfall (mean RF); (**b**) mean streamflow (Q_{mean}) versus mean rainfall for the 10 watersheds in the basin.

3.3.2. GR2M Model Performance

Moriasi et al. [52] recommend statistical ratings for evaluating the performance of a hydrologic model. The model calibration in the upland sub-basins (Near Holleta, Melka Kuntire, Hombole, and Mojo watersheds), Upper valley (Sire and Metehara), Middle valley (Melka Sedi and Kessem), and Lower Awash sub-basins (Adaitu and Tendaho) showed that model performance capabilities were "good" or higher. Furthermore, 80% and 17% of the calibrated *PBIAS* for gauged and satellite rainfall (TRMM 3B43v7 and PERSIANN-CDR) data showed a performance rating of "very good" and "good," respectively. The low-magnitude *PBIAS* in 80% of the calibrated watersheds indicates an accurate model simulation. The satellite rainfall data in the Metehara watershed exhibited a result of "satisfactory" compared to other watersheds in the basin (Table 4).

The model validation results indicate that 53% and 27% of the validated watersheds exhibited performance ratings of a model as "good" and "very good" when using *NSE* and *RSR* as evaluation criteria. Despite this, 20% were identified as unsatisfactory for integration with the GR2M model (Table 5).

Part of the Upper valley (Metehara watershed) and Middle valley (Sire watershed) sub-basins did not perform well with the GR2M model and scored an *NSE* of less than 50. However, the degree of collinearity between simulated and measured data was in the range of 0.58 to 0.64 in both watersheds, respectively.

A higher percentage of bias (*PBIAS*) was identified while validating the observed flow of the rivers using satellite rainfalls of some watersheds in a basin (Table 5). Higher *PBIAS* ($\geq \pm 25$) in Melka Kuntire (TRMM 3B43v7 and PERSIANN-CDR), Mojo (PERSIANN-CDR), Metehara (observed rainfall, TRMM 3B43v7 and PERSIANN-CDR), and Kessem (TRMM 3B43v7) watersheds were noted. The *NSE*, *RSR*, and R^2 values of these watersheds showed acceptable statistical results, with the exception of the Metehara and Melka Sedi watersheds. In the Melka Kuntire watershed, both satellite rainfall data underestimated the counterparts of the observed flow. Overestimations of simulated flows were detected in Mojo (PERSIANN-CDR), Metehara (all observed rainfall, TRMM 3B43v7, and PERSIANN-CDR), Kessem (observed rainfall), Adaitu (observed rainfall and PERSIANN-CDR), and Tendaho (observed and TRMM 3B43v7). The observed and satellite rainfall data exhibited underestimations in the majority of the watersheds in a basin using the GR2M model (Table 5).

The rainfall-streamflow hydrograph using the observed and the satellite rainfall products of the ARB are shown in Figures 7–9.

Table 4. Comparison of statistical evaluation criteria for the calibration of hydrologic data.

No.	Watershed	Rainfall Set	Calibration					
			NSE	*PBIAS*	R^2	*RSR*	Performance Rating	Remarks
1	Near Holleta	Observed	0.85	−3.03	0.85	0.38	Vg	Oe
		TRMM 3B43v7	0.77	−0.47	0.77	0.40	Vg	Oe
		PERSIANN-CDR	0.79	1.45	0.79	0.46	Vg	Ue
2	Melka Kuntire	Observed	0.87	−3.27	0.87	0.37	Vg	Oe
		TRMM 3B43v7	0.80	6.91	0.81	0.44	Vg	Ue
		PERSIANN-CDR	0.85	9.20	0.85	0.39	Vg	Ue
3	Hombole	Observed	0.80	11.06	0.78	0.49	Vg	Ue
		TRMM 3B43v7	0.82	2.89	0.82	0.42	Vg	Ue
		PERSIANN-CDR	0.83	−2.66	0.84	0.41	Vg	Oe
4	Mojo	Observed	0.90	9.51	0.90	0.31	Vg	Ue
		TRMM 3B43v7	0.83	10.48	0.86	0.41	Vg	Ue
		PERSIANN-CDR	0.78	−4.80	0.79	0.47	Vg	Oe
5	Sire	Observed	0.80	−1.84	0.80	0.44	Vg	Oe
		TRMM 3B43v7	0.80	−0.25	0.81	0.45	Vg	Oe
		PERSIANN-CDR	0.82	2.73	0.82	0.50	Vg	Ue
6	Metehara	Observed	0.76	3.36	0.77	0.49	Vg	Ue
		TRMM 3B43v7	0.60	0.93	0.63	0.63	S	Ue
		PERSIANN-CDR	0.56	7.79	0.59	0.66	S	Ue
7	Melka Sedi	Observed	0.76	3.92	0.76	0.49	Vg	Ue
		TRMM 3B43v7	0.76	−4.34	0.77	0.49	Vg	Oe
		PERSIANN-CDR	0.71	2.92	0.71	0.54	G	Ue
8	Kessem	Observed	0.93	7.24	0.93	0.27	Vg	Ue
		TRMM 3B43v7	0.87	−18.68	0.92	0.36	Vg	Oe
		PERSIANN-CDR	0.87	−12.40	0.88	0.36	Vg	Oe
9	Adaitu	Observed	0.70	0.79	0.72	0.79	G	Ue
		TRMM 3B43v7	0.73	4.67	0.76	0.52	G	Ue
		PERSIANN-CDR	0.85	0.39	0.89	0.39	Vg	Ue
10	Tendaho	Observed	0.68	2.78	0.69	0.56	G	Ue
		TRMM 3B43v7	0.74	−12.11	0.76	0.51	G	Oe
		PERSIANN-CDR	0.77	−10.68	0.82	0.48	Vg	Oe

Vg: very good; G: good; S: satisfactory; Oe: overestimation; Ue: underestimation.

Table 5. Comparison of statistical evaluation criteria for validation of hydrologic data.

No.	Watershed	Rainfall Set	Validation					
			NSE	*PBIAS*	R^2	*RSR*	Performance Rating	Remarks
1	Near Holleta	Observed	0.75	14.60	0.76	0.50	G	Ue
		TRMM 3B43v7	0.74	4.78	0.75	0.51	G	Ue
		PERSIANN-CDR	0.69	13.16	0.75	0.56	G	Ue
2	Melka Kuntire	Observed	0.63	19.13	0.65	0.61	S	Ue
		TRMM 3B43v7	0.73	34.24	0.86	0.52	G	Ue
		PERSIANN-CDR	0.76	26.27	0.81	0.49	Vg	Ue
3	Hombole	Observed	0.75	14.68	0.83	0.50	G	Ue
		TRMM 3B43v7	0.87	12.11	0.88	0.36	Vg	Ue
		PERSIANN-CDR	0.75	16.20	0.78	0.48	Vg	Ue
4	Mojo	Observed	0.70	7.34	0.74	0.55	G	Ue
		TRMM 3B43v7	0.82	3.69	0.82	0.44	Vg	Ue
		PERSIANN-CDR	0.67	−31.03	0.81	0.57	G	Oe
5	Sire	Observed	0.69	14.44	0.79	0.55	G	Ue
		TRMM 3B43v7	0.68	4.80	0.73	0.56	G	Ue
		PERSIANN-CDR	0.62	9.37	0.67	0.62	S	Ue
6	Metehara	Observed	0.34	−27.23	0.59	0.81	NS	Oe
		TRMM 3B43v7	0.34	−29.76	0.57	0.81	NS	Oe
		PERSIANN-CDR	0.46	−25.13	0.59	0.73	NS	Oe
7	Melka Sedi	Observed	0.42	23.60	0.64	0.76	NS	Ue
		TRMM 3B43v7	0.39	9.04	0.63	0.78	NS	Ue
		PERSIANN-CDR	0.40	7.44	0.58	0.78	NS	Ue
8	Kessem	Observed	0.65	−2.96	0.67	0.59	S	Oe
		TRMM 3B43v7	0.60	33.81	0.68	0.62	S	Ue
		PERSIANN-CDR	0.61	24.04	0.64	0.70	S	Ue
9	Adaitu	Observed	0.76	−0.57	0.85	0.49	Vg	Oe
		TRMM 3B43v7	0.79	10.44	0.82	0.46	Vg	Ue
		PERSIANN-CDR	0.65	−2.39	0.73	0.53	S	Oe
10	Tendaho	Observed	0.70	−23.37	0.77	0.54	G	Oe
		TRMM 3B43v7	0.62	−24.67	0.68	0.62	S	Oe
		PERSIANN-CDR	0.51	4.20	0.52	0.70	S	Ue

Vg: very good; G: good; S: satisfactory; Oe: overestimation; Ue: underestimation; NS: not satisfactory.

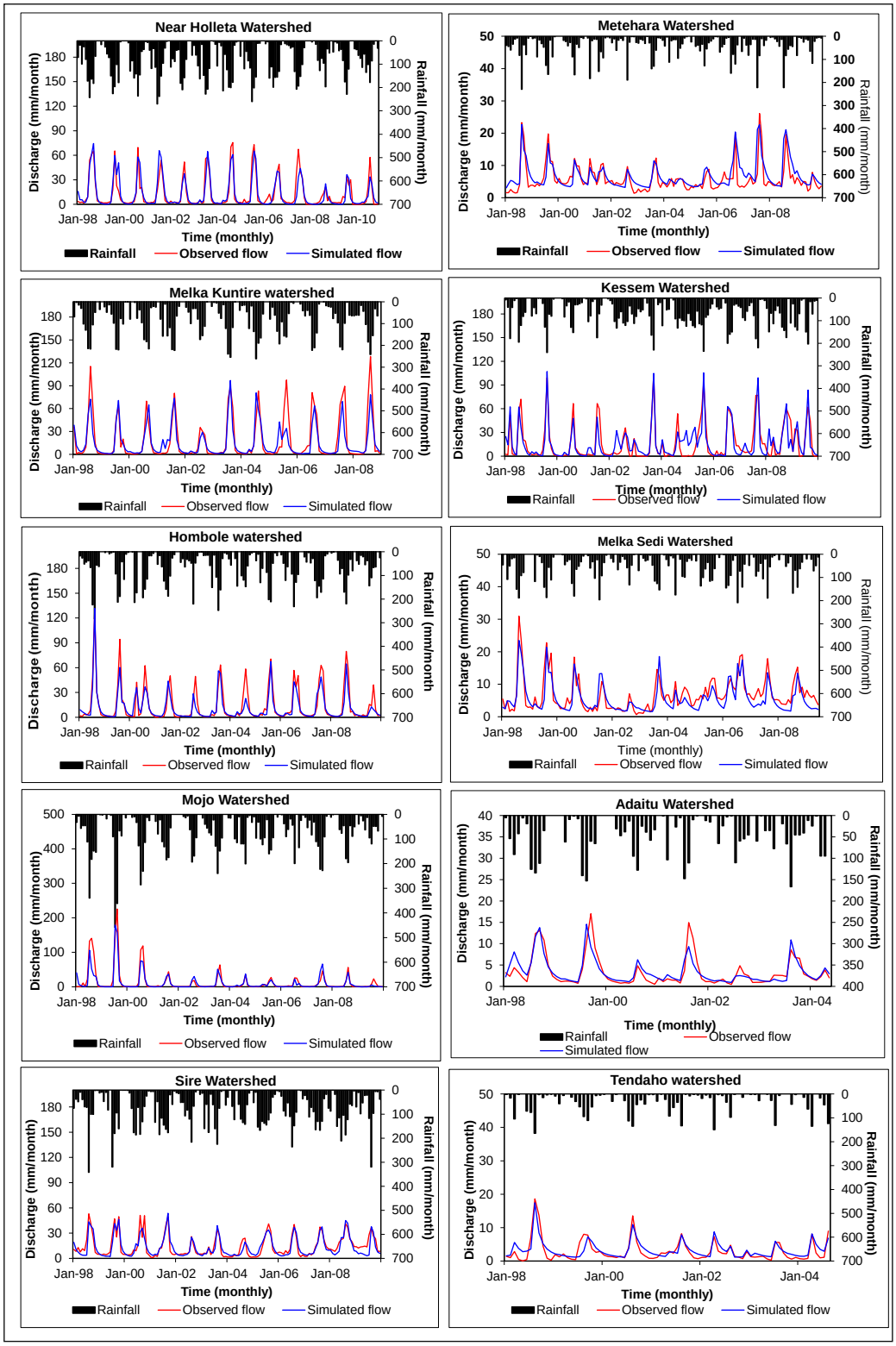


Figure 7. Calibration and validation procedure using gauged observed rainfall and streamflow records of the ARB.

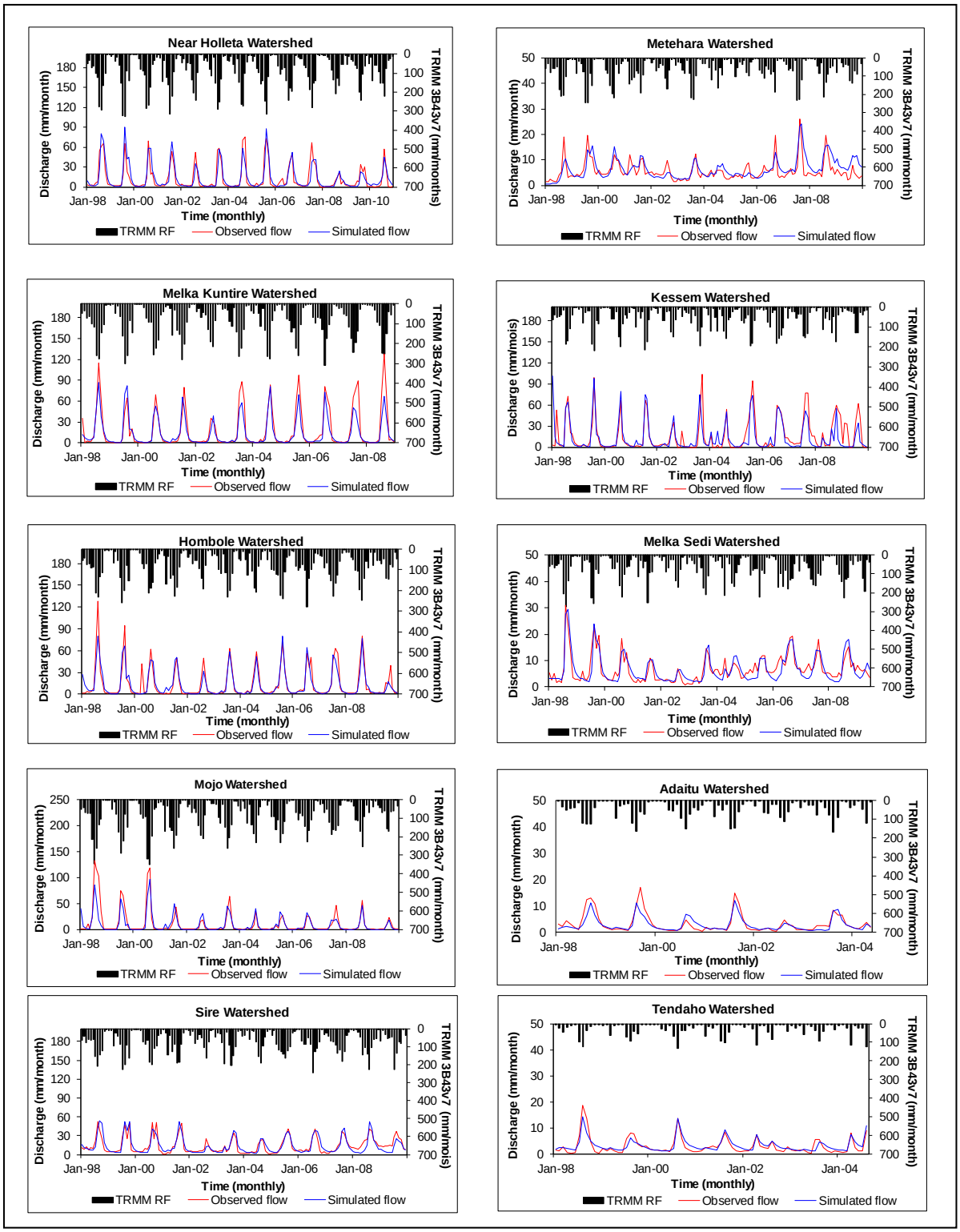


Figure 8. Calibration and validation procedure using Tropical Rainfall Measuring Mission (TRMM 3B43v7) rainfall and gauged streamflow records of the ARB.

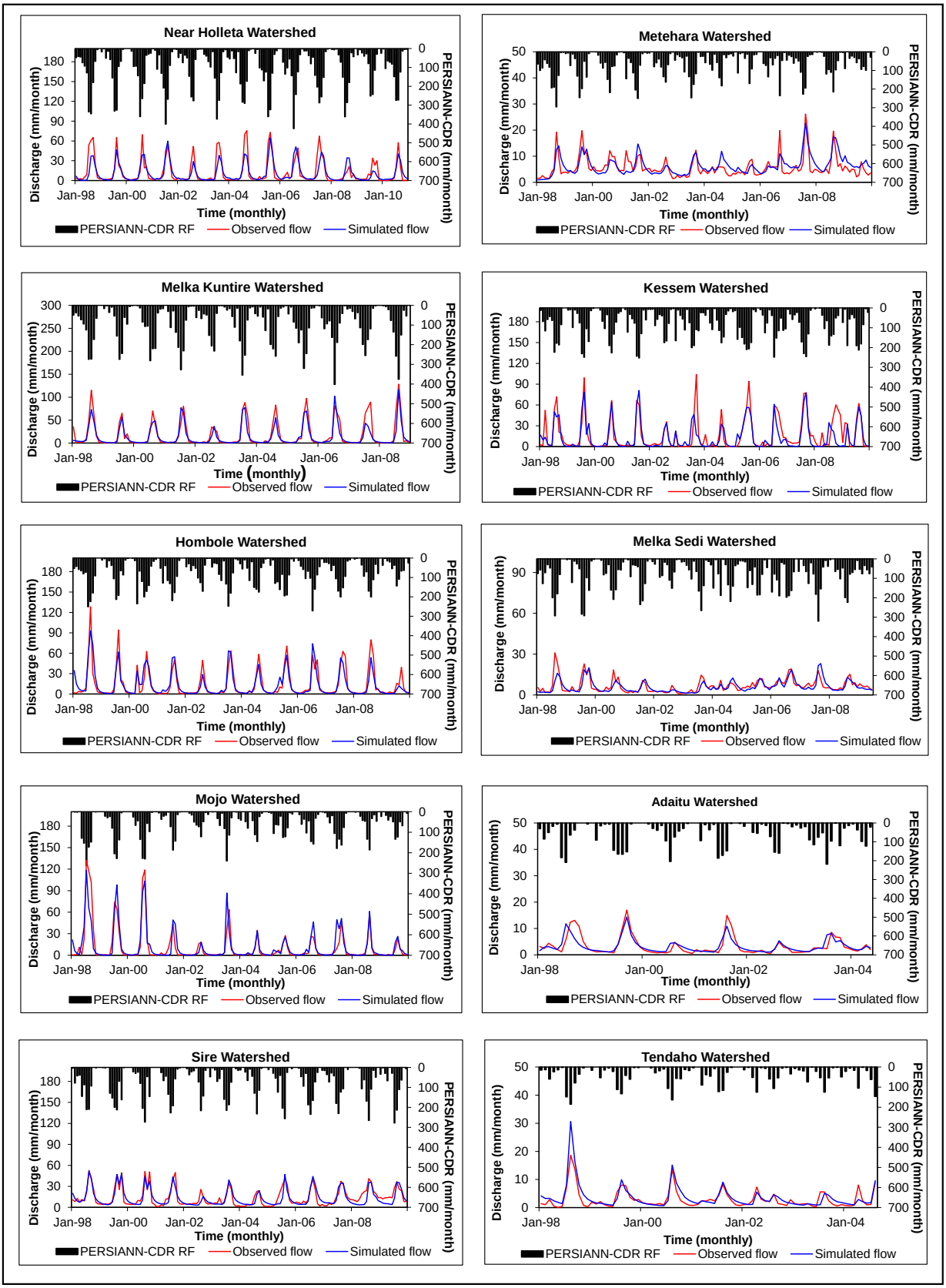


Figure 9. Calibration and validation procedure using Precipitation Estimation from Remotely Sensed Information using Artificial Neural Networks-Climate Data Record (PERSIANN-CDR) rainfall and gauged streamflow records of the ARB.

3.4. Discussion

Previously, different authors made intensive studies on rainfall-runoff modeling in Ethiopian river basins using various hydrologic models. These models can be distributed, semi-distributed, or lumped hydrologic models. As stated in the introduction section, SWAT, HBV, HEC-RAS, and other hydrologic models were tested and commonly recommended to use in different river basins of Ethiopia. The choice of these models may depend on the availability of the data or input requirement, topographic nature, climatic situations, soil type, land use, morphological characteristics of a watershed, and other related factors. The finding of this GR2M lumped water balance model provides better performance in ARB, except for some watersheds that require correction of the satellite rainfall data with higher *PBIAS*. The orographic effect in mountainous areas, rainfall regime and nature of the satellite rainfall products might affect the quality of satellite rainfall estimates and contributes to the variation in estimates of the product which later has an impact on rainfall-runoff modeling. Therefore, careful observation in the trends and amounts of satellite rainfall estimations versus elevation must be given due attention. Dinku et al. [35] suggested the variation in satellite rainfall estimation could be minimized through local calibration of satellite algorithms with remotely retrieved data and merging with ground-observed data as one technique. In general, evaluating this two-parameter water balance model in the ARB provides good alternative options for water resource planning in data-scarce regions of Ethiopia.

4. Conclusions and Recommendations

In this study, two satellite rainfall products and the observed rainfall from gauging stations were integrated with the GR2M hydrological water balance model over the complex and diverse terrain of the ARB in Ethiopia. The major findings of this study are as follows:

- Both satellite rainfall estimations showed a higher *PCC* with areal observed rainfall in the Uplands, the Western highlands, and the Lower sub-basins. However, the correlations in the Upper valley and the Eastern catchments of the basin were weak. Therefore, the satellite rainfall data in a watershed that are weakly associated need to be bias-corrected to improve the performance for integration with the GR2M model.
- The findings of the assimilated satellite rainfall products with GR2M model exhibited that 80% of the calibrated and 60% of the validated watersheds in a basin had lower magnitude of *PBIAS* ($<\pm 10$), which resulted in better accuracy in flow simulation.
- The hydrologic model validation results revealed that 80% of the validated watersheds using observed and satellite rainfall data sets showed a "good" or higher performance rating when the *NSE* and *RSR* were used as evaluation criteria. In contrast, 20% of them were unsatisfactory for integration with the GR2M model.
- The *PBIAS* results showed that the majority of the rainfall dataset of the watershed (73%) underestimated the simulated flow while integrating with the GR2M model. A higher *PBIAS* value, indicating unsatisfactory results, was observed only in the Melka Kuntire (TRMM 3B43v7 and PERSIANN-CDR), Mojo (PERSIANN-CDR), Metehara (all rainfall data set), and Kessem (TRMM 3B43v7) watersheds.
- Integrating these satellite rainfall data, particularly in data-scarce basins, with hydrological data generally appears to be useful in the environmentally diversified climate and topography of ARB. However, this requires validation with the ground-observed data.
- In general, this conceptual lumped model displayed better performance in majority of the ARB parts and is recommended to be tested in other river basins of Ethiopia for effective water resource planning and management.

Author Contributions: Conceptualization, G.B.A. and B.A.H.; methodology, G.B.A. and B.A.H.; software, G.B.A.; validation, G.B.A. and B.A.H.; formal analysis, G.B.A., B.A.H. and B.M.G.; investigation, G.B.A., B.A.H. and B.M.G.; resources, G.B.A., C.S., and W.-K.L.; data curation, G.B.A. and B.A.H.; writing—original draft preparation, G.B.A. and B.A.H.; writing—review and editing, G.B.A., B.A.H.,

B.M.G., C.S., and W.-K.L.; visualization, G.B.A., B.A.H., B.M.G., C.S., and W.-K.L.; supervision, G.B.A. and W.-K.L.; project administration, G.B.A.; funding acquisition, G.B.A., and W.-K.L. All authors have read and agreed to the published version of the manuscript.

Funding: This research received no external funding.

Institutional Review Board Statement: Not applicable.

Informed Consent Statement: Not applicable.

Data Availability Statement: Not applicable.

Acknowledgments: The authors gratefully acknowledge the support of the OJEong Resilience Institute (OJERI) at Korea University, the National Meteorological Agency of Ethiopia, Ministry of Water, Irrigation and Electricity (MoWIE) of Ethiopia, the Global Runoff Data Center (GRDC), National Meteorological Agency of Ethiopia (NMA), NASA Earth data (https://giovanni.gsfc.nasa.gov/giovanni/ accessed on 5 March 2020), and Center for Hydrometeorology and Remote Sensing (https://chrsdata.eng.uci.edu/ accessed on 15 March 2020). This research did not receive any specific grant from funding agencies in the public, commercial, or not-for-profit sectors.

Conflicts of Interest: The authors declare no conflict of interest. This research did not receive any specific grant from funding agencies in the public, commercial, or not-for-profit sectors.

References

1. Pande, S.; Savenije, H.H.G.; Bastidas, L.A.; Gosain, A.K. A Parsimonious hydrological model for a data scarce dryland region. *Water Resour. Manag.* **2011**, *26*, 909–926. [CrossRef]
2. Tarawneh, E.; Bridge, J.; Macdonald, N. A pre-calibration approach to select optimum inputs for hydrological models in data-scarce regions. *Hydrol. Earth Syst. Sci.* **2016**, *20*, 4391–4407. [CrossRef]
3. Dinku, T. Challenges with availability and quality of climate data in Africa. In *Extreme Hydrology and Climate Variability*; Melesse, A.M., Abtew, W., Senay, G.B., Eds.; Elsevier: Amsterdam, The Netherlands, 2019; pp. 71–80. ISBN 978-0-12-815998-9.
4. Tegegne, G.; Park, D.K.; Kim, Y.-O. Comparison of hydrological models for the assessment of water resources in a data-scarce region, the upper blue nile river basin. *J. Hydrol. Reg. Stud.* **2017**, *14*, 49–66. [CrossRef]
5. Tegegne, G.; Park, D.K.; Kim, Y.; Kim, Y.-O. Selecting hydrologic modelling approaches for water resource assessment in the Yongdam watershed. *J. Hydrol.* **2017**, *56*, 155.
6. Dinku, T.; Ceccato, P.; Grover-Kopec, E.; Lemma, M.; Connor, S.J.; Ropelewski, C.F. Validation of satellite rainfall products over East Africa's complex topography. *Int. J. Remote Sens.* **2007**, *28*, 1503–1526. [CrossRef]
7. Hirpa, F.A.; Gebremichael, M.; Hopson, T. Evaluation of high-resolution satellite precipitation products over very complex terrain in ethiopia. *J. Appl. Meteorol. Clim.* **2010**, *49*, 1044–1051. [CrossRef]
8. Bekele, D.; Alamirew, T.; Kebede, A.; Zeleke, G.; Melesse, A.M. Land use and land cover dynamics in the Keleta watershed, Awash River basin, Ethiopia. *Environ. Hazards* **2018**, *18*, 246–265. [CrossRef]
9. Korecha, D.; Barnston, A.G. Predictability of june–september rainfall in ethiopia. *Mon. Weather Rev.* **2007**, *135*, 628–650. [CrossRef]
10. Keraga, A.S.; Kiflie, Z.; Engida, A.N. Spatial and temporal water quality dynamics of Awash River using multivariate statistical techniques. *Afr. J. Environ. Sci. Technol.* **2017**, *11*, 565–577.
11. Nigatu Mersha, A.; de Fraiture, C.; Mehari, A.; Masih, I.; Alamirew, T. Integrated water resources management: Contrasting principles, policy, and practice, Awash River Basin, Ethiopia. *Water Policy* **2016**, *18*, 335–354. [CrossRef]
12. Castiglioni, S.; Lombardi, L.; Toth, E.; Castellarin, A.; Montanari, A. Calibration of rainfall-runoff models in ungauged basins: A regional maximum likelihood approach. *Adv. Water Resour.* **2010**, *33*, 1235–1242. [CrossRef]
13. Ibrahim, B.; Wisser, D.; Barry, B.; Fowe, T.; Aduna, A. Hydrological predictions for small ungauged watersheds in the Sudanian zone of the Volta basin in West Africa. *J. Hydrol. Reg. Stud.* **2015**, *4*, 386–397. [CrossRef]
14. Montanari, A.; Castiglioni, S.; Castellarin, A. Calibration of rainfall-runoff models in ungauged basins: A regional approach. *AGUFM* **2009**, *2009*, H21F-0911.
15. Dakhlaoui, H.; Ruelland, D.; Tramblay, Y.; Bargaoui, Z. Evaluating the robustness of conceptual rain-fall-runoff models under climate variability in northern Tunisia. *J. Hydrol.* **2017**, *550*, 201–217. [CrossRef]
16. Niel, H.; Paturel, J.-E.; Servat, E. Study of parameter stability of a lumped hydrologic model in a context of climatic variability. *J. Hydrol.* **2003**, *278*, 213–230. [CrossRef]
17. Coron, L.; Thirel, G.; Delaigue, O.; Perrin, C.; Andréassian, V. The suite of lumped GR hydrological models in an R package. *Environ. Model. Softw.* **2017**, *94*, 166–171. [CrossRef]
18. Folton, N.; Lavabre, J. Regionalization of a monthly rainfall-runoff model for the southern half of France based on a sample of 880 gauged catchments. *IAHS Publ.* **2006**, *307*, 264.
19. Makhlouf, Z.; Michel, C. A two-parameter monthly water balance model for French watersheds. *J. Hydrol.* **1994**, *162*, 299–318. [CrossRef]

20. Casimiro, W.S.L.; Labat, D.; Guyot, J.L.; Ronchail, J.; Ordonez, J.J. TRMM rainfall data estimation over the Peruvian Amazon-Andes basin and its assimilation into a monthly water balance model. In Proceedings of the New Approaches to Hydrological Prediction in Datasparse Regions, Proceedings of Symposium HS, Hyderabad, India, 6–12 September 2009; Volume 2, pp. 207–216.
21. Rau, P.; Bourrel, L.; Labat, D.; Ruelland, D.; Frappart, F.; Lavado, W.; Dewitte, B.; Felipe, O. Assessing multidecadal runoff (1970–2010) using regional hydrological modelling under data and water scarcity conditions in Peruvian Pacific catchments. *Hydrol. Process.* **2019**, *33*, 20–35. [CrossRef]
22. Lyon, S.W.; King, K.; Polpanich, O.; Lacombe, G. Assessing hydrologic changes across the Lower Mekong Basin. *J. Hydrol. Reg. Stud.* **2017**, *12*, 303–314. [CrossRef]
23. Zolfaghari, M.; Mahdavi, M.; Rezaei, A.; Salajegheh, A. Evaluating GR2M model in some small watersheds of Iran (Case study Gilan and Mazandaran Provinces). *J. Basic Appl. Sci. Res.* **2013**, *3*, 463–472.
24. Bachir, S.; Nouar, B.; Hicham, C.; Azzedine, H.; Larbi, D. Application of GR2M for rainfall-runoff modeling in Kébir Rhumel Watershed, north east of Algeria. *World Appl. Sci. J.* **2015**, *33*, 1623–1630.
25. Boulariah, O.; Longobardi, A.; Meddi, M. Statistical comparison of nonlinear rainfall-runoff models for simulation in Africa North-West semi-arid areas. In Proceedings of the 15th International Conference on Environment Science and Technology, Rhodes, Greece, 31 August–2 September 2017.
26. Nounangnonhou, T.C.; Fifatin, F.; Lokonon, B.E.; Acakpovi, A.; Sanya, E.A. Modelling and prediction of Ouémé (Bénin) river flows by 2040 based on GR2M approach. *LARHYSS J.* **2018**, *33*, 71–91.
27. Ibrahim, B.; Karambiri, H.; Polcher, J. Hydrological Impacts of the changes in simulated rainfall fields on nakanbe basin in burkina faso. *Climate* **2015**, *3*, 442–458. [CrossRef]
28. Tadesse, A.; Dai, W. Prediction of sedimentation in reservoirs by combining catchment based model and stream based model with limited data. *Int. J. Sediment Res.* **2019**, *34*, 27–37. [CrossRef]
29. Setegn, S.G.; Srinivasan, R.; Dargahi, B. Hydrological Modelling in the Lake Tana Basin, Ethiopia Using SWAT Model. *Open Hydrol. J.* **2008**, *2*, 49–62. [CrossRef]
30. Mekonnen, M.A.; Wörman, A.; Dargahi, B.; Gebeyehu, A. Hydrological modelling of Ethiopian catchments using limited data. *Hydrol. Process.* **2009**, *23*, 3401–3408. [CrossRef]
31. Uhlenbrook, S.; Mohamed, Y.; Gragne, A.S. Analyzing catchment behavior through catchment modeling in the Gilgel Abay, Upper Blue Nile River Basin, Ethiopia. *Hydrol. Earth Syst. Sci.* **2010**, *14*, 2153–2165. [CrossRef]
32. Abdo, K.S.; Fiseha, B.M.; Rientjes, T.H.M.; Gieske, A.S.M.; Haile, A.T. Assessment of climate change impacts on the hydrology of Gilgel Abay catchment in Lake Tana Basin, Ethiopia. *Hydrol. Process.* **2009**, *23*, 3661–3669. [CrossRef]
33. Rodriguez, E.; Sanchez, I.; Duque, N.; Lopez, P.; Kaune, A.; Werner, M.; Arboleda, P. Combined use of local and global hydrometeorological data with regional and global hydrological models in the Magdalena-Cauca river basin, Colombia. In Proceedings of the EGU General Assembly Conference Abstracts, Vienna, Austria, 23–28 April 2017; p. 10477.
34. National Meteorology Agency of Ethiopia Meteorological Station Information. Available online: http://www.ethiomet.gov.et/stations/information (accessed on 19 May 2020).
35. Dinku, T.; Connor, S.J.; Ceccato, P. Comparison of CMORPH and TRMM-3B42 over mountainous regions of Africa and South America. In *Satellite Rainfall Applications for Surface Hydrology*; Gebremichael, M., Hossain, F., Eds.; Springer: Dordrecht, The Netherlands, 2010; pp. 193–204.
36. Li, X.; Zhang, Q.; Xu, C.-Y. Assessing the performance of satellite-based precipitation products and its de-pendence on topography over Poyang Lake basin. *Theor. Appl. Climatol.* **2014**, *115*, 713–729. [CrossRef]
37. Stisen, S.; Sandholt, I. Evaluation of remote-sensing-based rainfall products through predictive capability in hydrological runoff modelling. *Hydrol. Process.* **2010**, *24*, 879–891. [CrossRef]
38. Gella, G.W. Statistical evaluation of high resolution satellite precipitation products in arid and semi-arid parts of Ethiopia: A note for hydro-meteorological applications. *Water Environ. J.* **2018**, *33*, 86–97. [CrossRef]
39. Romilly, T.G.; Gebremichael, M. Evaluation of satellite rainfall estimates over Ethiopian river basins. *Hydrol. Earth Syst. Sci.* **2011**, *15*, 1505–1514. [CrossRef]
40. Adeba, D.; Kansal, M.L.; Sen, S. Assessment of water scarcity and its impacts on sustainable development in Awash basin, Ethiopia. *Sustain. Water Resour. Manag.* **2015**, *1*, 71–87. [CrossRef]
41. Adane, G.B.; Hirpa, B.A.; Lim, C.-H.; Lee, W.-K. Spatial and temporal analysis of dry and wet spells in up-per awash river basin, ethiopia. *Water* **2020**, *12*, 3051. [CrossRef]
42. Karimi, P.; Bastiaanssen, W.G.M. Spatial evapotranspiration, rainfall and land use data in water accounting—Part 1: Review of the accuracy of the remote sensing data. *Hydrol. Earth Syst. Sci.* **2015**, *19*, 507–532. [CrossRef]
43. Adane, G.B.; Hirpa, B.A.; Song, C.; Lee, W.-K. Rainfall Characterization and Trend Analysis of Wet Spell Length across Varied Landscapes of the Upper Awash River Basin, Ethiopia. *Sustain. J. Rec.* **2020**, *12*, 9221. [CrossRef]
44. Ngongondo, C.; Xu, C.-Y.; Gottschalk, L.; Alemaw, B. Evaluation of spatial and temporal characteristics of rainfall in Malawi: A case of data scarce region. *Theor. Appl. Clim.* **2011**, *106*, 79–93. [CrossRef]
45. Searcy, J.K.; Hardison, C.H. *Double-Mass Curves. Manual of Hydrology: Part I, General Surface Water Techniques*; United States Government Printing Office: Washington, DC, USA, 1960; Volume 1541, pp. 31–40.
46. Food Agriculture Organization. *Report on the Agro-Ecological Zones Project*; FAO: Rome, Italy, 1978.

47. Zingore, S.; Murwira, H.K.; Delve, R.J.; Giller, K.E. Soil type, management history and current resource allocation: Three dimensions regulating variability in crop productivity on African smallholder farms. *Field Crop. Res.* **2007**, *101*, 296–305. [CrossRef]
48. Allen, R.G.; Pereira, L.S.; Raes, D.; Smith, M. *Crop Evapotranspiration-Guidelines for Computing Crop Water Requirements-FAO Irrigation and Drainage Paper 56*; FAO: Rome, Italy, 1998.
49. Verelst, L.; Wiberg, D. *HWSD Viewer Version 1.21*; FAO: Rome, Italy; IIASA: Luxemburg, Austria, 2012.
50. Mouelhi, S.; Madani, K.; Lebdi, F. A structural overview through GR(s) Models characteristics for better yearly runoff Simulation. *Open J. Mod. Hydrol.* **2013**, *3*, 179–187. [CrossRef]
51. Mouelhi, S.; Michel, C.; Perrin, C.; Andréassian, V. Stepwise development of a two-parameter monthly water balance model. *J. Hydrol.* **2006**, *318*, 200–214. [CrossRef]
52. Moriasi, D.N.; Arnold, J.G.; Van Liew, M.W.; Bingner, R.L.; Harmel, R.D.; Veith, T.L. Model evaluation guide-lines for systematic quantification of accuracy in watershed simulations. *Trans. ASABE* **2007**, *50*, 885–900. [CrossRef]
53. Nash, J.E.; Sutcliffe, J. V River flow forecasting through conceptual models part I—A discussion of principles. *J. Hydrol.* **1970**, *10*, 282–290. [CrossRef]
54. Thirel, G.; Andréassian, V.; Perrin, C.; Audouy, J.-N.; Berthet, L.; Edwards, P.; Folton, N.; Furusho, C.; Kuentz, A.; Lerat, J.; et al. Hydrology under change: An evaluation protocol to investigate how hydrological models deal with changing catchments. *Hydrol. Sci. J.* **2015**, *60*, 1184–1199. [CrossRef]